

# Necessary Condition to Utilize Adaptive Control in Wind Turbine Systems to Improve Power System Stability

Javad Taherahmadi, Mohammad Jafarian, Mohammad Naser Asefi

**Abstract**—The global capacity of wind power has dramatically increased in recent years. Therefore, improving the technology of wind turbines to take different advantages of this enormous potential in the power grid, could be interesting subject for scientists. The doubly-fed induction generator (DFIG) wind turbine is a popular system due to its many advantages such as the improved power quality, high energy efficiency and controllability, etc. With an increase in wind power penetration in the network and with regard to the flexible control of wind turbines, the use of wind turbine systems to improve the dynamic stability of power systems has been of significance importance for researchers. Subsynchronous oscillations are one of the important issues in the stability of power systems. Damping subsynchronous oscillations by using wind turbines has been studied in various research efforts, mainly by adding an auxiliary control loop to the control structure of the wind turbine. In most of the studies, this control loop is composed of linear blocks. In this paper, simple adaptive control is used for this purpose. In order to use an adaptive controller, the convergence of the controller should be verified. Since adaptive control parameters tend to optimum values in order to obtain optimum control performance, using this controller will help the wind turbines to have positive contribution in damping the network subsynchronous oscillations at different wind speeds and system operating points. In this paper, the application of simple adaptive control in DFIG wind turbine systems to improve the dynamic stability of power systems is studied and the essential condition for using this controller is considered. It is also shown that this controller has an insignificant effect on the dynamic stability of the wind turbine, itself.

**Keywords**—Almost strictly positive real, doubly-fed induction generator, simple adaptive control, subsynchronous oscillations, wind turbine.

## I. INTRODUCTION

ADAPTIVE control is a control that changes towards optimized performance in response to process dynamics and confusion. The aim of using adaptive control is that the controller be able to respond appropriately towards slight changes in the system and also modeling errors [1]. Simple adaptive control has the same structure as the common Proportional-Integral (PI) controller, but an adaption mechanism tends the PI parameters to optimum values. The difference between adaptive control and resistant control is that an adaptive control does not require knowing the system's

working period or level of parameter error [2].

Using an adaptive controller in order to improve the system's dynamic performance has been studied in various research efforts. In [3], an Improved Simple Adaptive Controller (ISAC) has been used in the AVR of the system synchronous generator in order to improve the networks small-signal stability. It has been shown that this controller has better performance in various system operating conditions, compared to common linear PSS. In [4], adaptive control has been used in the synchronous generator AVR system in order to increase the steady state stability of France's network.

Although this control has its advantages, there are restrictions on the use of simple adaptive control. For example, *the necessary condition for the convergence of simple adaptive control is that the system should be Almost Strictly Positive Real (ASPR). It has been proven that if the controlled system be ASPR, SAC will be convergent. The sufficient condition for being ASPR is that all zeroes and poles of the system should be at the left-hand side of the imaginary axis [5].* The test system used for the simulations in this paper does not qualify this condition, but, it is shown that by utilizing a parallel feedforward compensator, this condition can be satisfied. Case studies are used to evaluate the impact of this additional block parameter on the dynamic performance of the wind turbine and its contribution to network subsynchronous damping.

Subsynchronous resonance (SSR) is one of the undesirable and detrimental dynamic phenomena in power networks [6]. These oscillations are the result of energy conversion between the turbine-synchronous generator system and the electrical network in one or a number of frequencies, and they have the ability to damage the rotor of synchronous generators. SSR usually occurs in series capacitor compensated networks and is addressed in three categories according to IEEE standards as: induction generator effect, torsional interaction effect, and torque amplification [7].

With regard to the damaging effects of SSR in power systems, various methods have been proposed for a reduction of SSR in power systems to date. As an example in [8], [9], implementation of the Static synchronous series compensator in reducing the networks SSR is evaluated, and in [10] it is shown

Javad Taherahmadi is with the Department of Environment and Energy, Science and Research Branch of Islamic Azad University, Tehran, Iran (e-mail: j\_taherahmadi@yahoo.com).

Mohammad Naser Asefi is with the Department of Electrical Engineering, Islamic Azad University of Ashtian, Ashtian, Iran.

Mohammad Jafarian is with the Power Electrical Engineering, Niroo Research Institute, Tehran, Iran.

that HVDC converters can be controlled to improve the network subsynchronous oscillations.

With increasing wind power penetration in power networks, research on the effect of wind farms on the dynamic stability of power systems is of great significance. The doubly-fed induction generators (DFIGs) are more popular compared to other wind turbines due to their flexible control system [11]. With regard to the high influence and increasing trend of these turbines in the network and also with regard to their flexible controllability, the application of these turbines in improving dynamic conditions of the power system have been extensively studied.

Using DFIG-based wind turbines to damp power system subsynchronous oscillations has been the subject of recent researches. In [12] the performance of the Fuzzy Logic Damping Controller (FLDC) and Conventional Damping Controller (CDC) have been compared as extra controller loops in DFIG for damping system subsynchronous oscillations. In [13], a supplementary control loop has been used in the grid side converter of the DFIG to damp system Subsynchronous oscillations. In [14], in addition to studying the potential of SSR damping by DFIG converters, selecting the appropriate feedback-signal has been discussed.

Whereas the network dynamic conditions change constantly (with regard to various system operating conditions) and with regard to the fact that the DFIG rotor's speed changes at a wide range (with regard to changes in wind speed), using a linear

control loop in the DFIG structure cannot guarantee optimum performance in reducing the network SSR at all wind speeds and all network operating conditions; since linear control is designed at one specific point.

In this paper, adaptive control theory is used to design an auxiliary control loop for DFIGs, to damp system subsynchronous oscillations. Since the adaptive control parameters have the tendency towards optimum values with changes in system conditions, this controller provides optimized performance in various system operating conditions and wind speeds.

## II. STUDY SYSTEM AND MODELING OF DFIG

In this section the study system will be initially introduced and then modeling of the DFIG wind farm will be presented.

### A. Introduction of the Study System

In this paper, the IEEE first benchmark model for computer simulation of subsynchronous resonance was chosen as the study system [15]. This system includes a transmission line which connects an 892.4 MVA synchronous generator to an infinite-bus. Fig. 1 presents the single line diagram of this system. In this figure, the per-unit impedances are in the MVA base of the generator.

The generator's mechanical system includes a four stage steam turbine, a generator, and an excitation system. The parameters of this network have been introduced in [15].

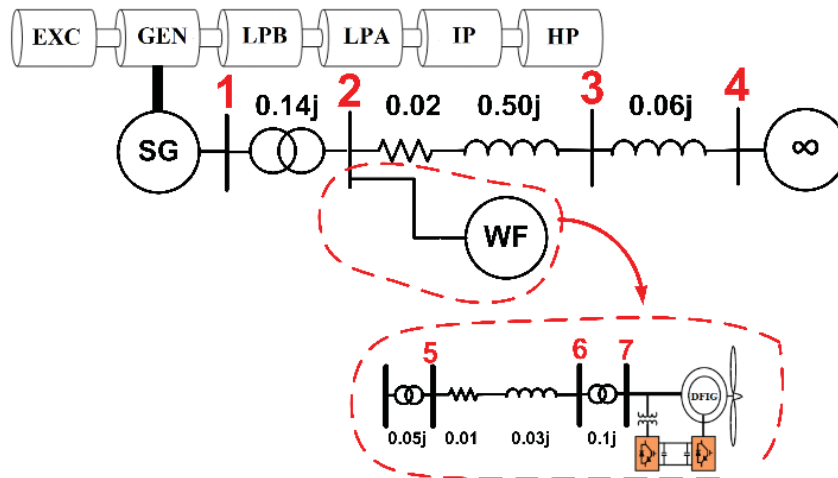


Fig. 1 IEEE first benchmark model for evaluating SSR

### B. Modeling the Wind Farm

It is assumed that a 350 MW DFIG-based wind farm is connected to the network. Various studies have shown that to study the effect of wind farms on the network dynamics, the aggregated model can be used for the wind farm [16], [17]. The aggregated model of the wind farm used in this study is depicted in Fig. 1 (impedances are presented in per-unit on the base of wind farm capacity) [18].

### C. Modeling DFIG Turbine

Modeling the DFIG turbine includes modeling the turbine,

DFIG generator and turbine controllers.

**Turbine:** Wind turbines convert kinetic energy in the wind into mechanical power. The mechanical torque generated by the turbine is calculated by [19]:

$$T_m = \frac{\rho \pi D^2 C_p V_w^3}{2\omega_r} \quad (1)$$

where,  $T_m$  is the turbine's mechanical torque,  $\rho$  is the wind density,  $D$  is length of the turbine blade,  $C_p$  is the power coefficient,  $V_w$  the wind speed,  $\omega_r$  is the rotor torsional speed.

In this study, in order to model the power coefficient of the turbine, the model used in [20] has been applied. In this reference, the turbine power coefficient has been modeled as:

$$C_p = 0.22(116/\lambda - 0.4\beta - 5) \exp(-12.5/\lambda) \quad (2)$$

In which,  $\lambda = D\omega_t/V_w$  is the tip-speed ratio and  $\beta$  is the blade pitch.

**Generator:** The dynamic equations of the doubly fed generator have been modeled by transferring equations of three-phase voltage to a synchronous d-q axis [21].

**Drive Train System:** In order to model the drive train system of the wind turbine, a two-mass model has been used (one mass for the turbine and one mass for the generator) [22].

**Turbine Controllers:** The DFIG wind turbine controller is comprised of two separate sections:

- ✓ Wind turbine controller: with the aim of absorbing the most wind power, by controlling the pitch angle and also limiting the turbine power at high wind speeds.
- ✓ Generator Controller: with the aim of controlling the real and reactive power generation of the generator and also limiting the voltages and currents of the generator. The generator controllers are comprised of two controllers; the Grid Side Converter (GSC) and the Rotor Side Converter (RSC) [12].

In variable speed wind turbines, the pitch control strategy is commonly used in order to maximize the turbine power generation at low and average wind speeds, and protect the turbine at high wind speeds [23]. While the blade pitch is equal to zero, the highest energy absorption is obtained. By increasing the blade pitch, wind absorption power is decreased. In Fig. 2 (a), the block diagram of blade pitch control and its interaction with the turbine-generator system is depicted [24]. According to this figure, the blade pitch is controlled using a PI controller, such that the generator rotor speed tracks the reference rotor speed in steady state. In this figure,  $K_{i6}$  and  $K_{p6}$  are control gains and  $T_p$  shows the step motor delay used for changing the turbines blade pitch. In this figure,  $V_w$  is wind speed,  $\beta$  is blade pitch,  $P_m$  indicates turbine mechanical power,  $P_e$  is the generator electrical power,  $\omega_r$  is the rotation speed of generator,  $\omega_t$  is the turbine rotation speed, and  $\omega_{ref}$  is the reference generator speed.

If the stator leakage reactance is neglected, it can be shown that the active power of the DFIG ( $P$ ) is proportional to the q-axis rotor current; and its reactive power ( $Q$ ) is proportional to the d-axis rotor current. That is, the turbine active power can be controlled by  $i_{qr}$  and its reactive power can be controlled by  $i_{dr}$ . This can be implemented by two PI controllers. On the other hand, it can be shown that  $i_{qr}$  can be controlled by the q-axis rotor voltage ( $u_{qr}$ ) and  $i_{dr}$  can be controlled by the d-axis rotor voltage ( $u_{dr}$ ), which can be implemented by two PI controllers [21]. This control strategy is shown in Fig. 2 (b). In this figure,  $P^*$  and  $Q^*$  are active power and the reactive power reference signal, respectively, and  $K_{p1}$ ,  $K_{i1}$ , ...,  $K_{i4}$  are the rotor side PI gains. Also in this figure,  $P_{WF}$  and  $Q_{WF}$  are the active and reactive power of the wind turbine.

Whereas voltage control mode is common in wind farms with high capacity, only this mode has been modeled in this

study. In this control mode, the reference voltage ( $u^*$  in Fig. 2 (b)) is determined by the operator. In this diagram,  $T_R$ ,  $T_S$  and  $T_c$  are signal transmission and implementation delays,  $K_{i5}$  and  $K_{p5}$  are the PI gains to regulate wind farm voltage and  $u_{reg}$  is the voltage of the voltage-control-bus.  $P_{SAC}$  is the supplementary control loop output that will be presented in the next part.

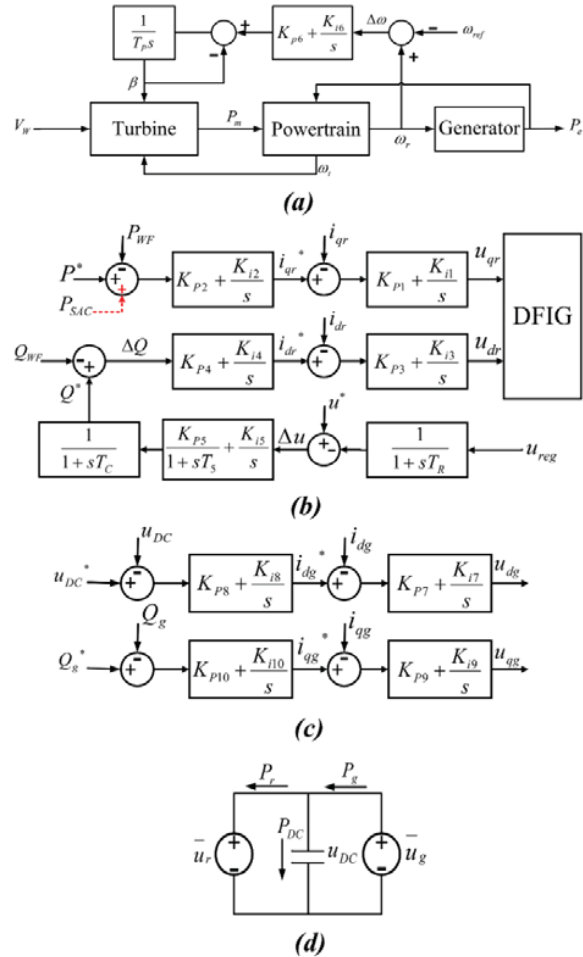


Fig. 2 (a) Block diagram of Blade pitch control, (b) Block diagram of rotor side converter control, (c) Block diagram of the grid side converter control, (d) Block diagram of the DC link

The grid side converter is modeled as a voltage source. In this converter, the aim is to regulate the DC link voltage and set the consumed reactive power of the converter equal to zero (in order to reduce the converter size) [25]. Fig. 2 (c) shows the block diagram of the grid side converter control [26]. In this figure,  $Q_g$  is the converter reactive power,  $u_{DC}$  is the DC link voltage,  $u_{DC}^*$  and  $Q_g^*$  are the reference signal of the DC link voltage and the converter reactive power,  $i_{dg}$  is the d-axis current of the GSC,  $i_{qg}$  is the q-axis current of the GSC,  $u_{dg}$  and  $u_{qg}$  are d-axis and q-axis voltage of the GSC, respectively, while  $K_{p7}$ ,  $K_{i7}$ , ...,  $K_{i10}$  are GSC PI control gains.

The DC link can be modeled by (3). In this equation, the g and r index indicate parameters related to GSC and RSC,

respectively; and  $u_{DC}$  and  $C$  indicate voltage and capacitance of the DC link capacitor, respectively. Fig. 2 (d) shows the block diagram of the DC link.

$$Cu_{DC} \frac{d}{dt} u_{DC} = P_r - P_g \tag{3}$$

$$P_r = u_{qr} i_{qr} + u_{dr} i_{dr}$$

$$P_g = u_{qg} i_{qg} + u_{dg} i_{dg}$$

**Supplementary Controllers:** If the supplementary control is added to the active power control loop in RSC, the active power modulation is obtained, while adding it to the reactive power control loop leads to reactive power modulation [27]. Previous research studies indicate that both modulations are effective and

have acceptable effects on the damping of various subsynchronous oscillations [28]. In this paper only active power modulation is carried out.

Selecting the appropriate feedback signal for the supplementary control loop has an important role in designing damping control loops [29], [30]. Also, its proven that synchronous-generator rotors speed includes almost all torsional modes of system and in most of the articles published in this field, the rotor speed deviation is used as the input signal of damping controller [31]-[33]. Therefore, this signal is chosen as the input for the supplementary control loops.

Using the supplementary controller in the DFIG control structure and its interaction with the system has been shown in Fig. 3 (a). The structure of this supplementary controller and its design are introduced in the following chapter.

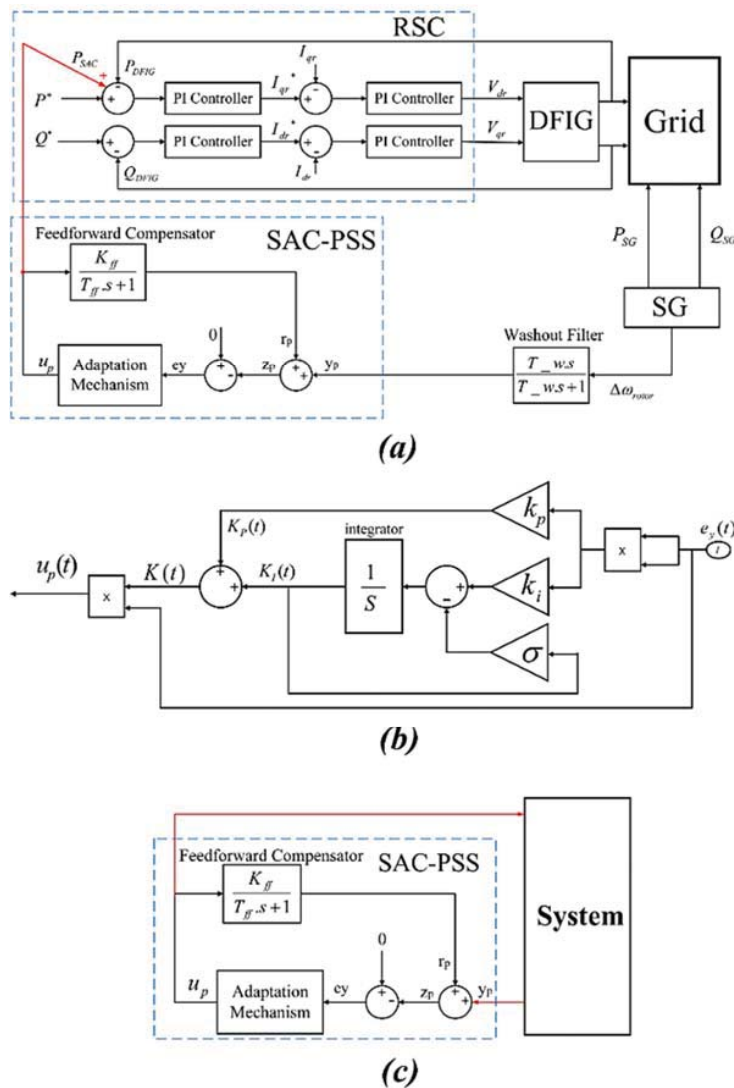


Fig. 3 (a) Block diagram of supplementary control loop, (b) Block diagram of SAC, (c) Block diagram of feed-forward compensator

III. DESIGN OF SUPPLEMENTARY CONTROL LOOP

In this paper, simple adaptive controller (SAC) is used which

is in fact a simplified version of the model reference adaptive control (MRAC) which is designed based on the command



generator tracker theory (MRAC-CGT) [34]. This control system is used to control a system described as:

$$\begin{aligned}\dot{x}_p(t) &= A_p x_p(t) + B_p u_p(t) \\ y_p(t) &= C_p x_p(t)\end{aligned}\quad (4)$$

where  $X_p(t)$  is the state vector,  $u_p(t)$  is the command vector and  $y_p(t)$  is the output vector of the system.  $A_p$ ,  $B_p$  and  $C_p$  are the matrices with appropriate dimensions. The equations of the reference model can be described as:

$$\begin{aligned}\dot{x}_m(t) &= A_m x_m(t) + B_m u_m(t) \\ y_m(t) &= C_m x_m(t)\end{aligned}\quad (5)$$

where  $X_m(t)$  is the state vector,  $u_m(t)$  is the command vector and  $y_m(t)$  is the output of the reference model.  $A_m$ ,  $B_m$  and  $C_m$  are the matrices with appropriate dimensions. The output tracking error can be defined as:

$$e_y(t) = y_m(t) - y_p(t) \quad (6)$$

By using the adaptive control mechanism defined in (7), the control vector of the controlled system ( $u_p(t)$ ) is produced such that without knowing the exact matrices  $A_p$ ,  $B_p$  and  $C_p$ ; the controlled system output ( $y_p(t)$ ) tend to the reference model output ( $y_m(t)$ ), and thus the error value ( $e_y(t)$ ) will be the least possible [34]. In (7),  $K_e$ ,  $K_x$ , and  $K_u$  are feedback-error gain, feedback-reference state gain and feedback-reference input gain, respectively.

$$\begin{aligned}u_p(t) &= K_e(t)e_y(t) + K_x(t)x_m(t) + K_u(t)u_m(t) \\ u_p(t) &= K(t).r(t)\end{aligned}\quad (7)$$

In this equation, feedback gains ( $K(t)$ ) and inputs ( $r(t)$ ) are defined as:

$$\begin{aligned}K(t) &= [K_e(t), K_x(t), K_u(t)] \\ r(t) &= [e_y(t), x_m(t), u_m(t)]\end{aligned}\quad (8)$$

Equation (9) explains the process to determine the time varying values of the feedback-gains ( $K(t)$ ) in SAC. According to this equation, ( $K(t)$ ) is itself comprised of two sections including a proportional gain ( $K_p$ ) and an integral gain ( $K_i$ ).

$$\begin{aligned}K(t) &= K_p(t) + K_i(t) \\ K_p(t) &= e_y(t).r^T(t).k_p \\ \dot{K}_i(t) &= e_y(t).r^T(t).k_i - \sigma.K_i(t)\end{aligned}\quad (9)$$

In this  $\sigma$  is introduced so that divergence of integral gains during turbulence is prevented.  $k_p$  and  $k_i$  are also the positive definite and positive semi-definite adaptive gains. Appropriate

values should be selected for  $\sigma$ ,  $k_p$  and  $k_i$  by the designer.

While our aim of employing SAC is damping out (or on other word vanishing) the subsynchronous oscillations, the reference model should actually be zero in our case. In this situation, (9) will be shortened as (10).

$$\begin{aligned}K(t) &= K_p(t) + K_i(t) \\ K_p(t) &= e_y^2(t).k_p \\ \dot{K}_i(t) &= e_y^2(t).k_i - \sigma.K_i(t)\end{aligned}\quad (10)$$

Fig. 3 (b) shows the modeling of the adaptive control loop with regard to (4)-(10).

#### IV. EVALUATING CONVERGENCE OF THE ADAPTIVE CONTROLLER

As mentioned in the introduction, if the controlled system be Almost Strictly Positive Real (ASPR), SAC will be convergent and sufficient condition for being ASPR is that all zeroes and poles of the system to be at the left-hand side of the imaginary axis. By evaluating the zeroes and poles of the system, it was noticed that the one pair of the system zeros are placed at the right-hand side of the imaginary axis and therefore the control system is not ASPR.

It can be proven that if the system is not ASPR, by using a parallel feed-forward compensator the system can be altered to an ASPR system [5]. Fig. 3 (c) shows the block diagram of the feed-forward compensator and its arrangement. The transfer function of the feed-forward block is simply considered as a gain ( $K_{ff}$ ) and a delay ( $T_{ff}$ ). In the event that the first-degree transfer function is not able to transform the system to ASPR, a higher degree transfer function should be used (which in our case was not necessary).

Fig. 4 shows the zeroes and poles of the system before and after using the feed-forward compensator at the wind speed of 12.5 meter per second (m/s) as an example. As it can be seen in this figure, the study system has a pair of zeroes at the right-hand side of the imaginary axis, which will be transferred to the left-hand side by using the feed-forward compensator in the system, and therefore the system becomes ASPR.

The parallel feed-forward block gains ( $K_{ff}$  and  $T_{ff}$ ) should be selected such that the system will remain ASPR in all of its working conditions. To do that, the values of these two parameters were changed from 0 to large amounts and the system's poles and zeros were calculated for three different wind speeds 11 m/s, 12.5 m/s, and 19 m/s; (corresponding to the subsynchronous, synchronous and super-synchronous operation modes of the DFIG wind turbine, respectively). Fig. 5 shows the permissible region to select the values of these two gains ( $K_{ff}$  and  $T_{ff}$ ).

Fig. 3 (a) shows the arrangement of SAC, parallel feed-forward compensator and their relationship with the DFIG turbine and power system. The wash-out filter blocks the low-frequency variations of generator-rotor speed to enter to the SAC, so that the SAC operates only for subsynchronous oscillations and does not operate in steady state. In this figure,

the feed-forward compensator is used in order to authenticate the ASPR conditions.

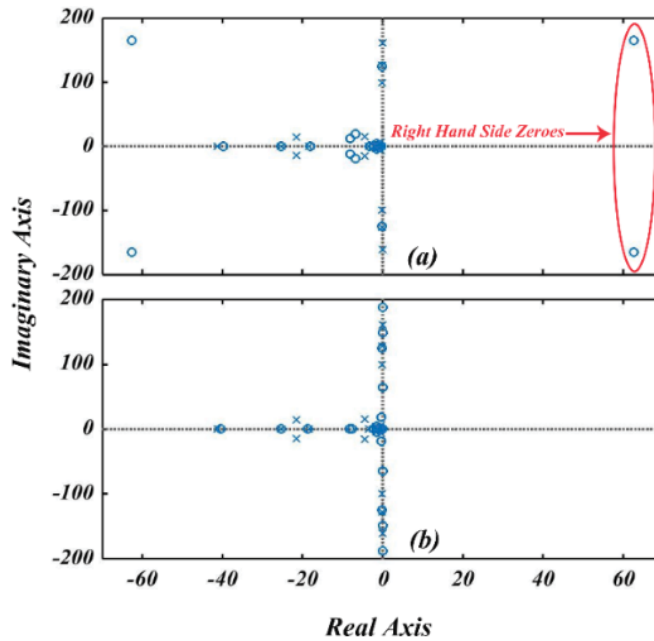


Fig. 4 System zeroes and poles at wind speed 12.5 m/s: (a) Without feed-forward compensator, (b) With feed-forward compensator

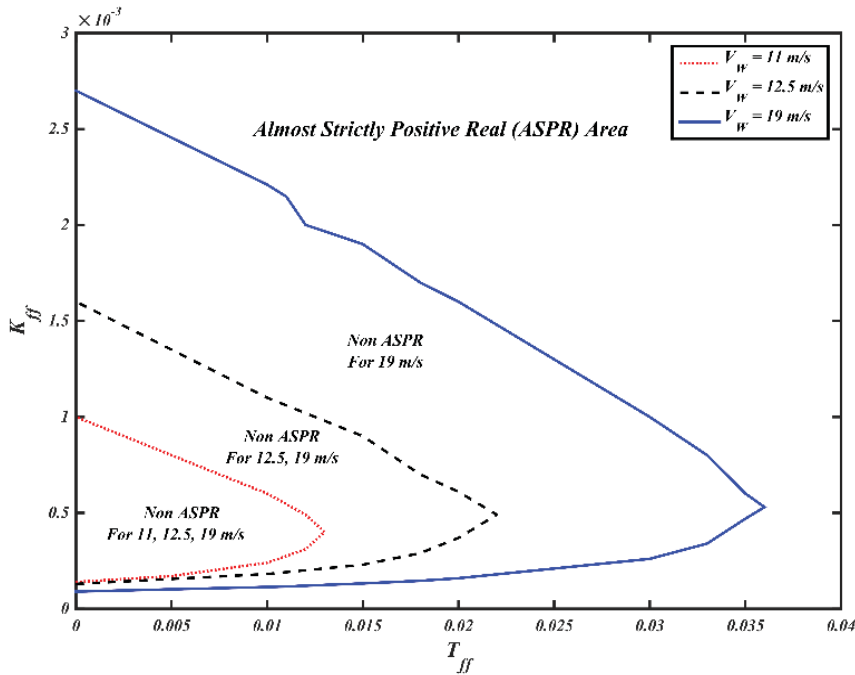


Fig. 5 The permissible region to select the feed-forward compensator gains

The feed-forward compensator gains ( $K_{ff}$  and  $T_{ff}$ ) along with SAC gains ( $k_p$ ,  $k_i$  and  $\delta$ ) should be selected properly, so that while the SAC damped out the network subsynchronous oscillations, it does not negatively affect the dynamic performance of the wind turbine itself. In this work, these gains are selected by trial and error.

#### V. SIMULATION RESULT

The MATLAB/Simulink software was used for modeling the DFIG turbine and simulation of the subsynchronous oscillations in the network. Simulations were carried out in wind speed of 12.5 meter per second.

In order to evaluate the network's subsynchronous

oscillations, a three-phase short circuit was implemented at the infinite-bus at  $t=0.01$  for three cycles. Then the effect of the SAC controller on damping the network subsynchronous oscillations was evaluated.

Fig. 6 shows the active power generation of the synchronous generator ( $P_{SG}$ ) with and without using SAC. This figure well depicts SSR damping, in the active power of the synchronous generator after using SAC.

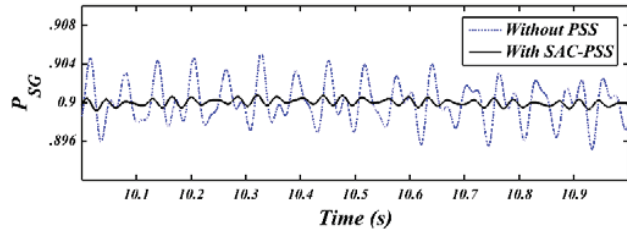


Fig. 6  $P_{SG}$  with and without using SAC

Fig. 7 shows the active power variations ( $P_{DFIG}$ ) of the DFIG wind farm before and after using SAC. As it can be seen, using the SAC at the control structure of the DFIG turbine has a negligible effect on the dynamic performance of the DFIG itself.

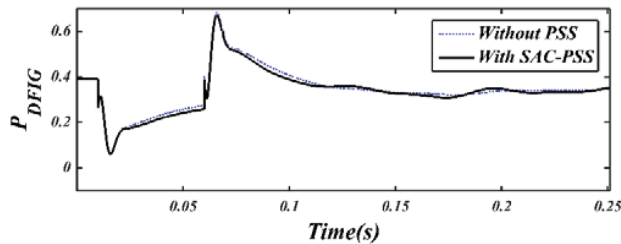


Fig. 7  $P_{DFIG}$  with and without using SAC

## VI. CASE STUDIES: THE EFFECT OF SELECTING SAC GAINS

In this section, the effect of selecting SAC gains on the dynamic performance of both the study system and DFIG turbine is study. For this purpose, various amounts are assigned to the five main parameters of the designed adaptive control loops and simulations were carried out once more. The values of  $K_{ff}$  and  $T_{ff}$  are selected such that the system remains ASPR (with regard to Fig. 11).

Fig. 8 shows the effect of parallel feed-forward compensator gain ( $K_{ff}$ ) and the parallel feed-forward compensator time constant ( $T_{ff}$ ) on the network subsynchronous oscillations and Fig. 9 shows their effect on the wind turbines dynamic performance.

Considering the results of Figs. 8 and 9, the following results are concluded:

- The best value for  $K_{ff}$  and  $T_{ff}$  is approximately 1. Selecting these two parameters has a significant effect on how the SAC controller influences the network subsynchronous oscillations.
- Even though a decrease in  $K_{ff}$  from 1 and an increase of  $T_{ff}$  from 1 results in improving the network's subsynchronous

oscillations, at the same time it causes a negative effect on the dynamic performance of the wind farm.

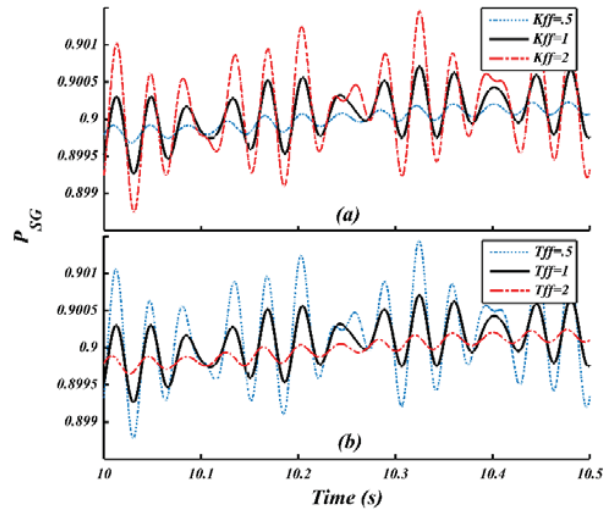


Fig. 8 Synchronous generator active power generation for various values of  $K_{ff}$  and  $T_{ff}$

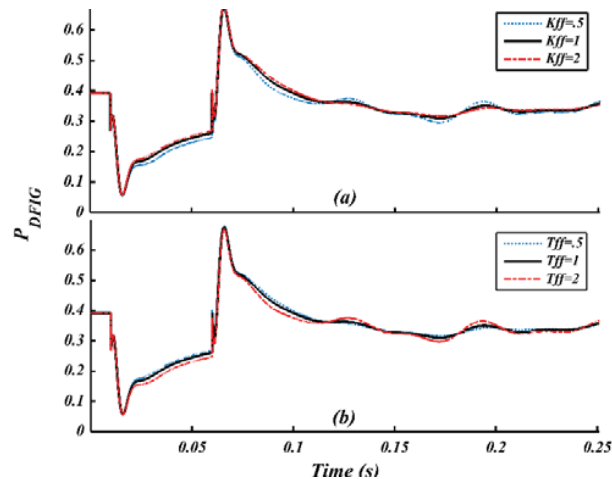


Fig. 9 Wind farm active power generation for various values of  $K_{ff}$  and  $T_{ff}$

Figs. 10 and 11 shows the effect of proportional gain ( $k_p$ ), integral gain ( $k_i$ ) and  $\delta$  on the dynamic performance of synchronous generator and wind farm active power generation, respectively. Considering these figures, it can be concluded that:

- Selecting the value of  $k_p$  on SAC performance practically has minor effect.
- Increasing the amount of  $k_i$  results in improving network Subsynchronous oscillations. This is while changes in  $k_i$  practically have minor effect on the wind farm dynamic performance.
- Decreasing  $\delta$  up to .01 results in improving subsynchronous resonance. This is while changes in  $\delta$  practically have minor effect on wind farm dynamic performance.

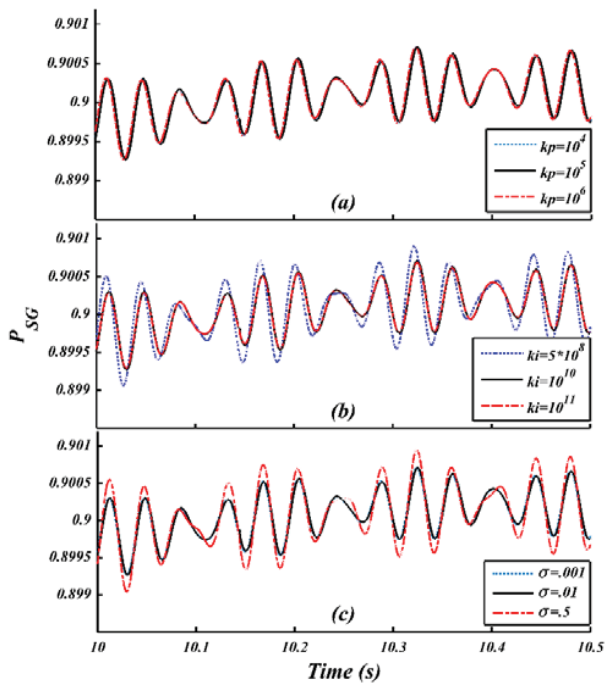


Fig. 10 Synchronous generator active power generation for various amounts of  $k_p$ ,  $k_i$ , and  $\bar{\sigma}$

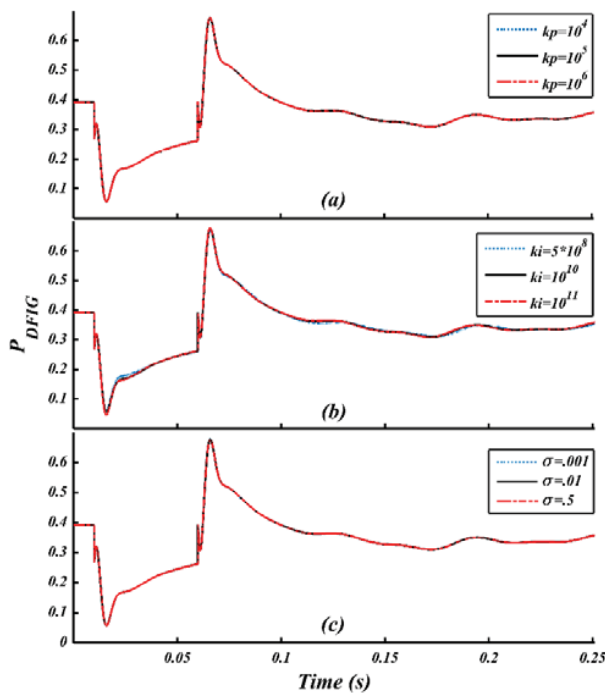


Fig. 11 Wind farm active power generation for various values of  $k_p$ ,  $k_i$ , and  $\bar{\sigma}$

## VII. CONCLUSION

This paper studied the necessary condition to utilize adaptive control in wind turbine systems to improve power system stability.

This was done by damping of the power network subsynchronous oscillations using a DFIG-based wind farm with adding a control loop to the rotor side convertor of the DFIG turbine. This control loop was designed by adaptive control theory. Using the adaptive controller resulted in the wind farm being more effective in enhancing damping of the network's subsynchronous oscillations in various operating conditions and different wind speeds.

The IEEE first benchmark model for evaluating subsynchronous resonance was used as the study system. It was assumed a 350 MW DFIG-based wind farm was connected to this network. The MATLAB/Simulink software was used for modeling the wind farm and simulating the network subsynchronous oscillations. Simulations were carried out in wind speed of 12.5 meter per second.

The condition for SAC convergence is that the control system should be ASPR. This is while the study system was not ASPR. In order to make the system to ASPR, a feed-forward compensator block is added to the system in parallel form and its parameter values are determined such that the system remains ASPR during various DFIG operating modes. Next, the adaptive control block is implemented and added to the active power control loop of rotor side controller in DFIG turbine. The generator-rotor speed variations were used as the input signal for the auxiliary control loop, as it has high participation in network SSR modes.

Synchronous generator and DFIG active power generation were simulated. It was noticed that using SAC in the DFIG-based wind turbine noticeably increase the damping of network subsynchronous oscillations at all the wind speeds.

In this paper, selection of adaptive controller parameter gains was done by trial and error. By considering an objective function, in which increasing of network SSR damping and improvement of dynamic performance of the wind farm was taken into consideration, optimum values of adaptive control parameters could be obtained using optimization methods. Also in this paper, only modulation of the active power of the rotor side convertor was evaluated. Modulation of the reactive power of the rotor side convertor or modulation of grid side convertor could be considered, which are currently being researched by the authors of this paper.

## REFERENCES

- [1] Landau I. D., Lozano R., M'Saad M. Adaptive control: Springer Berlin; 1998.
- [2] Åström K. J., Wittenmark B. Adaptive control: Courier Dover Publications; 2013.
- [3] Zhang, S., & Luo, F. L. An improved simple adaptive control applied to power system stabilizer. Power Electronics, IEEE Transactions on. 2009; 24(2), 369-375.
- [4] Irving, E., Barret, J., Charcossey, C., & Monville, J. Improving power network stability and unit stress with adaptive generator control. Automatica, 1979, 15(1), 31-46.
- [5] Barkana I, "Simple adaptive control—a stable direct model reference adaptive control methodology—brief survey," International Journal of Adaptive Control and Signal Processing, 2014, vol. 28, pp. 567-603.
- [6] Walker D. N., Bowler C. L., Jackson R. L., Hodges D. A. Results of subsynchronous resonance test at Mohave. IEEE Trans Power ApSyst 1975; 5:1878–89.
- [7] Group, I. S. R. W., Terms, definitions and symbols for subsynchronous oscillations, IEEE Trans. power Appl. Syst., 1985, PAS-104, 6, pp. 1325-



- 1334.
- [8] Al Jowder F. A. R., Ooi B-T. Series compensation of radial power system by a combination of SSSC and dielectric capacitors. *Power Delivery, IEEE Transactions on.* 2005;20(1):458-65.
- [9] Bongiorno M., Angquist L., Svensson J. A novel control strategy for subsynchronous resonance mitigation using SSSC. *Power Delivery, IEEE Transactions on.* 2008;23(2):1033-41.
- [10] De Toledo P. F., Ångquist L., Nee H.-P. Frequency-domain modelling of subsynchronous torsional interaction of synchronous machines and a high voltage direct current transmission link with line-commutated converters. *IET generation, transmission & distribution.* 2010;4(3):418-31.
- [11] Carlin P. W., Laxson A. X., Muljadi E. B. The history and state of the art of variable-speed wind turbine technology. *Natl Renew Energ Lab Tech Rep NREL/TP-500-28 607;* 2001.
- [12] Mokhtari, M., Khazaei, J., & Nazarpour, D. Subsynchronous resonance damping via doubly fed induction generator. *International Journal of Electrical Power & Energy Systems,* 2013, 53, 876-883.
- [13] Zhu, C., Fan, L., & Hu, M. Control and analysis of DFIG-based wind turbines in a series compensated network for SSR damping. Paper presented at the Power and Energy Society General Meeting, 2010 IEEE.
- [14] Fan L., Miao Z. Mitigating SSR using DFIG-based wind generation. *IEEE Trans Sustainable Energy* 2013; 3:349–58.
- [15] First benchmark model for computer simulation of subsynchronous resonance, *IEEE Trans. power Appl. Syst.,* 1977, PAS-96, 5, pp. 1565-1572.
- [16] Gautam, D., Vittal, V., Harbour, T., Impact of increased penetration of DFIG-based wind turbine generators on transient and small signal stability of power systems, *IEEE Trans. Power Syst.,* 2009, 24, 3, pp. 1426-1434.
- [17] Fan L., Kavasseri R., Miao Z., Zhu Ch. Modelling of DFIG-based wind farms for SSR analysis. *IEEE Trans Power Deliver* 2010; 25:2073–82.
- [18] Pourbeik, P., *Wind Farm Integration in British Columbia – Stages 1&2 : Planning and Interconnection Criteria,* ABB Report, 2005.
- [19] Manwell J. F., McGowan J. G., Rogers A. L., *Wind energy explained.* Amherst, USA: Wiley, 2002.
- [20] Yang L., Xu Z., Østergaard J., Dong Z. Y., and Wong K. P., "Advanced control strategy of DFIG wind turbines for power system fault ride through," *IEEE Trans. Power Syst.,* 2012, vol. 27, pp. 713-722.
- [21] Miao Z., Fan L. "The art of modelling and simulation of induction generator in wind generation applications using high-order model," *Simul. Pract. Theory,* 2008, vol. 16, pp. 1239-125.
- [22] Bianchi F. D., De Battista H., and Mantz R. J., *Wind turbine control systems: principles, modelling and gain scheduling design:* Springer Science & Business Media, 2006.
- [23] Yang L., Xu Z., Østergaard J., Dong Z. Y., Kit P. W., Ma X, Oscillatory stability and eigenvalue sensitivity analysis of A DFIG wind turbine system, *IEEE Trans. Energy Convers.,* 2011, 26, 1, pp. 328-339.
- [24] Pourbeik P. (convener), *Modelling and dynamic behavior of wind generation as it relates to power system control and dynamic performance,* International Council Large Electrical System (CIGRE), Technical Brochure WGC4.601, 2007.
- [25] Mei F., Pal B., Modal analysis of grid-connected doubly fed induction generators, *IEEE Trans. Energy Convers.,* 2007, 22, 3, pp. 728-736.
- [26] Fan L., Zhu Ch., Miao Z., Kavasseri R., Hu M. Modal analysis of a DFIG-based windfarms influenced with a series compensated network. *IEEE Trans EnergConvers* 2011; 26:1010–20.
- [27] Jafarian M, Ranjbar A. M. The impact of wind farms with doubly fed induction generators on power system electromechanical oscillations. *Renew Energ* 2012; 50:780–5.
- [28] Fan, L., Yin, H., & Miao, Z. On active/reactive power modulation of DFIG-based wind generation for interarea oscillation damping. *Energy Conversion, IEEE Transactions on.* 2011; 26(2), 513-521.
- [29] Farsangi M. M., Sung Y. H., Lee K. Y. Choice of FACTS device control inputs for damping interarea oscillations. *IEEE Trans Power Syst* 2004; 19:1135–43.
- [30] Magaji N., Mustafa M. W. Optimal location and signal selection of UPFC device for damping oscillation. *Electr Power EnergSyst* 2011; 33:1031–42.
- [31] Varma R. K., Auddy S., Semsedini Y. Mitigation of subsynchronous resonance in a series-compensated wind farm using FACTS controllers. *Power Delivery, IEEE Transactions on.* 2008;23(3):1645-54.
- [32] El-Moursi M. S., Bak-Jensen B., Abdel-Rahman M. H. Novel STATCOM controller for mitigating SSR and damping power system oscillations in a series compensated wind park. *Power Electronics, IEEE Transactions on.* 2010;25(2):429-41.
- [33] El-Moursi M. S. Mitigating subsynchronous resonance and damping power system oscillation in a series compensated wind park using a novel static synchronous series compensator control algorithm. *Wind Energy.* 2012;15(3):363-77.
- [34] Kaufman H., Barkana I., Sobel K., *Direct adaptive control algorithms,* Springer Verlag, New York, 1994.